

Reprinted from:

THE JOURNAL OF CHEMICAL PHYSICS

VOLUME 56, NUMBER 10

15 MAY 1972

Laser Magnetic Resonance Spectrum of NO_2 at 337 μm and 311 μm *

R. F. CURL, JR.

Chemistry Department, Rice University, Houston, Texas 77001

AND

K. M. EVENSON AND J. S. WELLS

Quantum Electronics Division, National Bureau of Standards, Boulder, Colorado 80302

(Received 31 January 1972)

The Zeeman components of several rotational transitions of nitrogen dioxide have been observed in absorption using the 311 and 337 μm lines of an HCN laser as a source. The Zeeman components of four rotational transitions (two at 311 μm and two at 337 μm) have been assigned. Two components of the g tensor have been determined from the spectrum by least square fitting. The anisotropic component $(aa)_g^{(S)}$, obtained as -0.010 , agrees well with that predicted from theory, but the isotropic component $(0)_g^{(S)}$, obtained as 2.013, does not agree satisfactorily with theoretical prediction or with solid phase measurements both of which give 1.9997. The rotational frequencies of the four transitions have also been obtained.

INTRODUCTION

In laser magnetic resonance spectroscopy the absorption of energy from a laser source is observed when the Zeeman components of a rotational (or in some cases vibrational) transition are swept over the laser frequency by varying the magnetic field in which the sample is placed. Laser magnetic resonance spectroscopy has been used to study O_2 ,¹ OH ,² CH ,³ and NO .⁴ This work is concerned with the paramagnetic asymmetric rotor, NO_2 .

The rotational spectrum of NO_2 has been studied previously.⁵⁻¹¹ The hyperfine coupling constants, molecular structure, and dipole moment were accurately determined. Reasonably good values of the centrifugal distortion constants have been obtained. From these studies it is possible to predict quite accurately the laser Zeeman spectrum. Such predictions have made the

assignment of the spectra reported here which arise from low N rotational states quite easy.

From analysis of the spectrum, information concerning the Zeeman Hamiltonian may be obtained. This work is a report of the observation, assignment, and analysis of this spectrum of NO_2 with a view towards determining as many constants of the Zeeman Hamiltonian as possible.

EXPERIMENTAL

The laser magnetic resonance spectrometer is shown in Fig. 1. The laser oscillates between mirrors C and D and is divided into two parts with the dielectric beam splitter. A valve (not shown) permits the connection of both sides for simultaneous evacuation in order to protect the beam splitter. The beam splitter can be rotated from the Brewster angle to increase the cou-

TABLE I. Carefully measured Zeeman components.

Assignment ^a			$H_{\text{obs}} - H_{\text{calc}}$ (G)		
	$M \rightarrow M'$	$i \rightarrow i'$	Field (G)	First least squares	Second least squares
337 μ					
$7_{1,7} \rightarrow 8_{2,6}$ $\Delta M = 0$	-11/2 \rightarrow -11/2	1 \rightarrow 4	1 011.6	-0.2	-0.4
	-13/2 \rightarrow -13/2	1 \rightarrow 5	1 058.8	-0.3	-0.2
$\Delta M = \pm 1$	-15/2 \rightarrow -15/2	1 \rightarrow 5	1 107.1	-0.3	0.1
	-9/2 \rightarrow -11/2	1 \rightarrow 4	1 008.3	0.3	-0.7
	-13/2 \rightarrow -15/2	2 \rightarrow 5	1 104.3	0.2	-0.3
	-15/2 \rightarrow -17/2	1 \rightarrow 3	1 185.0	0.3	1.4
$8_{1,7} \rightarrow 9_{2,8}$					
$\Delta M = 0$	5/2 \rightarrow 5/2	2 \rightarrow 4	1 698.5	-0.5	-0.1
	-15/2 \rightarrow -15/2	2 \rightarrow 6	2 115.3	-0.2	0.0
$\Delta M = \pm 1$	15/2 \rightarrow 17/2	1 \rightarrow 5	1 469.0	-0.0	-0.0
	3/2 \rightarrow 5/2	2 \rightarrow 6	1 689.2 ^b		
	3/2 \rightarrow 1/2	2 \rightarrow 6	1 745.3 ^b		
	-5/2 \rightarrow -7/2	1 \rightarrow 4	1 914.5	-0.0	-0.1
	-13/2 \rightarrow -15/2	1 \rightarrow 4	2 091.4	0.2	-0.4
	-13/2 \rightarrow -15/2	2 \rightarrow 5	2 099.2	0.2	-0.0
	-13/2 \rightarrow -15/2	3 \rightarrow 6	2 105.0	0.2	0.2
-17/2 \rightarrow -19/2	1 \rightarrow 3	2 204.6	0.4	0.3	
Unassigned $\Delta M = 0$			1 291.1		
			1 442.9		
311 μ					
$7_{2,6} \rightarrow 6_{3,3}$ $\Delta M = \pm 1$	7/2 \rightarrow 5/2	5 \rightarrow 2	2 746.2	5.0	+0.1
	-11/2 \rightarrow -9/2	5 \rightarrow 2	4 604.0	-5.1	-0.1
$6_{2,4} \rightarrow 5_{3,3}$ $\Delta M = \pm 1$	-5/2 \rightarrow -3/2	2 \rightarrow 5	5 394.4	6.7	+0.1
	-11/2 \rightarrow -9/2	2 \rightarrow 4	6 651.8	-7.0	-0.1
Unassigned $\Delta M = 0$			10 184.2		
			10 481.1		
			10 838.7		
$\Delta M = \pm 1$				10 261.1	
				10 645.9	
				11 114.4	
				11 199.8	
				11 722.3	

^a The quantum number i , designates which level of given M is referred to. The energy levels of given M are arranged in order of increasing energy with lowest energy having $i=1$.

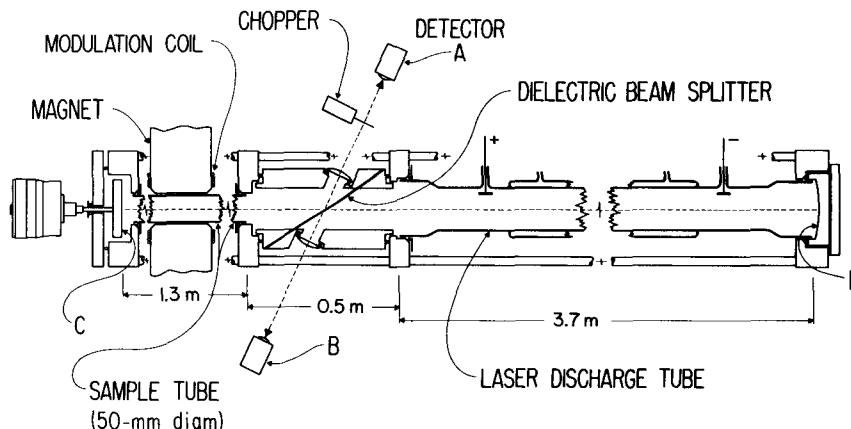
^b There are several lines with comparable intensity at this field. These lines were omitted from the fitting.

pling to the laser cavity. Standard quartz window Golay cells were used for the two detectors. Detector A was used to set the laser to the center of the laser line, and detector B fed the amplifier synchronized with the modulation coil. Full laser output of several milliwatts was incident on detector B. A 15 in. magnet with $5\frac{1}{2}$ in. Rose shimmed pole tips was used; it permitted fields to 23.5 kG. The modulation coil was driven at 83 Hz with an amplitude of 1.3 G. The magnetic field was precisely measured with an NMR gaussmeter and pre-

cision frequency counter. The field was measured simultaneously with the recording of the spectra by placing the NMR probe outside the sample tube adjacent to the pole cap of the magnet. A correction for the difference between the magnetic field at the position of the NMR probe and the field at the sample position was then made to the data. The previously measured frequencies of the 337 and 311 μm lines were 890 760.7 and 964 313.4 MHz.¹²

The NO_2 resonance was observed at pressures of ap-

FIG. 1. Diagram of the laser magnetic resonance apparatus. The laser cavity is formed by mirrors C and D. The sample (in this case NO₂) is confined to the vacuum chamber to the left of the beam splitter. The laser discharge is to the right of the beam splitter.



proximately 5 torr. At these pressures the Zeeman components observed were not appreciably power saturated and the linewidths were approximately 1 G. The laser radiation is polarized by the beam splitter and the orientation of the plane of polarization could be made either perpendicular or parallel to the magnetic field H_0 by rotating the entire beam splitter assembly about the laser axis.

OBSERVATIONS

The observed transitions are electric dipole transitions and therefore the parallel transitions ($\Delta M_F = 0$) are found for the laser electric field E_ω , parallel to the Zeeman field H_0 . For the perpendicular orientation the selection rules are, of course, $\Delta M_F = \pm 1$.

Confirmation of the electric dipole nature of the transitions is given by the observation that there are more lines observed when the electric field of the laser radiation is perpendicular to Zeeman field than when it is parallel [e.g., see Fig. 2(b)]. This is expected for electric dipole transitions because $E_\omega \perp H_0$ corresponds to $\Delta M = \pm 1$, and $E_\omega \parallel H_0$ corresponds to $\Delta M = 0$. For magnetic dipole transitions $H_\omega \perp H_0$ corresponds to $\Delta M = \pm 1$ and $H_\omega \parallel H_0$ corresponds to $M = 0$.

The observed spectra are shown in Figs. 2 and 3. In Fig. 2(a), a wide scan of the field is used so that a general impression of the spectra can be formed. As can be seen, the spectra generally consist of groups of lines. Each group corresponds to a rotational transition. Rotational quantum numbers have been assigned to four low N transitions and are indicated on Fig. 2(a). The only absorption observed but not shown on Fig. 2(a) was observed at just above 10 kG at 311 μm and is shown on an expanded field scale in Fig. 2(b). The region between 0 and 2.5 kG at 337 μm was also recorded on an expanded scale and is shown in Figs. 3(a) and 3(b). As can be seen a wealth of hyperfine structure can be resolved.

The magnetic field at the absorption center was

measured carefully for a number of lines. These are reported in Table I.

THEORY

The theory of the hyperfine splittings of asymmetric rotors with an odd number of electrons has been discussed by several authors.^{13,14} The Zeeman effect of the similar molecule ClO₂ has been observed and analyzed.¹⁵ Because the Zeeman effect of ClO₂ was observed only at very low fields (~ 10 G), the Zeeman Hamiltonian could be much simplified. For the large fields used here it seems most appropriate to write down a relatively complete Zeeman Hamiltonian and then to decide which terms may affect the spectrum.

Accordingly we write

$$\hat{H} = \hat{H}_{\text{rot}} + \hat{H}_0 + \hat{H}_Z, \quad (1)$$

where \hat{H}_{rot} is the rotational Hamiltonian and would include the effects of centrifugal distortion as well as the rigid rotor, \hat{H}_0 is the hyperfine Hamiltonian which is already well known.⁹ \hat{H}_Z is the Zeeman Hamiltonian and has the form

$$\hat{H}_Z = (\hat{H}_S + \hat{H}_N + \hat{H}_I) \cdot \mathbf{H} - \frac{1}{2} \mathbf{H} \cdot \hat{\chi} \cdot \mathbf{H}, \quad (2)$$

where \mathbf{H} is the applied magnetic field, \hat{H}_S describes the interaction of the electron spin with the field, \hat{H}_N describes the interaction of the rotational magnetic moment with the field, \hat{H}_I describes the interaction of the nuclear spin of ¹⁴N with the field, and $\hat{\chi}$ is the diamagnetic susceptibility tensor (see Huttner, Lo, and Flygare¹⁶ for a treatment of $\hat{\chi}$)

$$\hat{H}_S \cdot \mathbf{H} = \mu_B \mathbf{S} \cdot \hat{\mathbf{g}}^{(S)} \cdot \mathbf{H}, \quad (3)$$

$$\hat{H}_N \cdot \mathbf{H} = -\mu_N \hat{\mathbf{N}} \cdot \hat{\mathbf{g}}^{(N)} \cdot \mathbf{H}, \quad (4)$$

$$\hat{H}_I \cdot \mathbf{H} = -\mu_N g_I (\hat{\mathbf{I}} \cdot \mathbf{H}), \quad (5)$$

where μ_B is the Bohr magneton, μ_N is the nuclear mag-

TABLE II. Approximate contributions of terms of the Zeeman Hamiltonians.

Parameter	Approximate magnitude of parameter MHz/G	Approximate contribution to energy in MHz ^b (at 1000 G)	Apparent shift in field at which transition occurs in G
$\mu_B(0)_g^{(S)}$	2.8	2800	...
$\mu_B(aa)_g^{(S)}$	0.01	10	4
$\mu_B(cc)_g^{(S)}$	0.01	10	4
$\mu_N(0)_g^{(N)}$	0.001	1	0.4
$\mu_N(aa)_g^{(N)}$	0.001	1	0.4
$\mu_N(cc)_g^{(N)}$	0.001	1	0.4
μ_{NGI}	0.0005	0.5	0°
χ	10^{-8} ^a	0.01	4×10^{-3}

^a MHz/(G)²^b Crudely estimated as $10^3 \times$ first column. For χ ; $10^6 \times$ first column.^c For all the transitions observed $\Delta M_I = 0$ and g_I cancels out in frequency.

neton, and g_I is the nuclear g factor of ^{14}N . The quantities \hat{g}^S and \hat{g}^N are the electron spin and rotational g tensors, respectively.

The two g tensors \hat{g}^S and \hat{g}^N may be further reduced into an isotropic and a quadrupolar part. Thus in the principal axis system of the molecule

$$\hat{H}_S \cdot \mathbf{H} = \mu_B \{ (0)_g^{(S)} (\hat{\mathbf{S}} \cdot \mathbf{H}) + (aa)_g^{(S)} \hat{S}_a \hat{H}_a + (bb)_g^{(S)} \hat{S}_b \hat{H}_b + (cc)_g^{(S)} \hat{S}_c \hat{H}_c \}, \quad (6)$$

$$\hat{H}_N \cdot \mathbf{H} = -\mu_N \{ (0)_g^{(N)} (\hat{\mathbf{N}} \cdot \mathbf{H}) + (aa)_g^{(N)} \hat{N}_a \hat{H}_a + (bb)_g^{(N)} \hat{N}_b \hat{H}_b + (cc)_g^{(N)} \hat{N}_c \hat{H}_c \}, \quad (7)$$

with the requirements

$$(aa)_g^{(S)} + (bb)_g^{(S)} + (cc)_g^{(S)} = 0, \quad (8a)$$

$$(aa)_g^{(N)} + (bb)_g^{(N)} + (cc)_g^{(N)} = 0. \quad (8b)$$

The $\hat{g}^{(S)}$ tensor may be estimated from the spin rotation coupling constants.^{6,17}

Having written down a fairly complete Zeeman Hamiltonian, it now is time to consider the magnitude of the various terms. A very crude estimate of the contribution of each term is given in Table II. The ultimate purpose is to decide which terms of the Zeeman Hamiltonian Eq. (2) can be determined from the laser Zeeman spectrum. On considering Table II it appears impossible to determine χ and g_I and probably quite difficult to determine $g^{(N)}$. From Table II it appears possible to determine $g^{(S)}$. This question must be considered more carefully later in the analysis of the observations.

SPECTRUM PREDICTION COMPUTATION

Before attempting to determine $g^{(S)}$ it is necessary to assign the observed spectrum. From Table II it can be concluded that this may be done using the simple Zeeman Hamiltonian

$$H_Z = 2\mu_B (\hat{\mathbf{S}} \cdot \mathbf{H}). \quad (9)$$

Accordingly, a computer program was written to

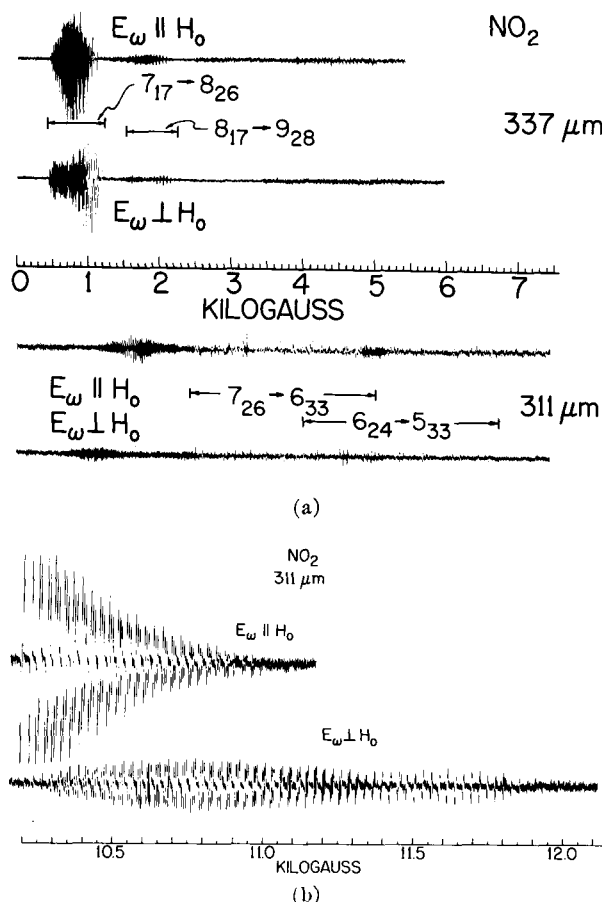


Fig. 2. (a) Observed laser Zeeman spectra of NO_2 . The upper two traces show the observed absorptions (first derivative display) when the laser is tuned to $337 \mu\text{m}$ ($890\,760.7 \text{ MHz}$). The lower two traces show the observed absorption when the laser is tuned to $311 \mu\text{m}$ ($964\,313.4 \text{ MHz}$). At each frequency the upper trace corresponds to the electric vector of the plane polarized radiation parallel to the magnetic field ($\Delta M = 0$ selection rules) and the bottom trace to laser electric vector perpendicular to the magnetic field ($\Delta M = \pm 1$ selection rules). The only strong absorption system observed but not shown in this figure is found just above 10 kG at $311 \mu\text{m}$ and is shown on an expanded scale in Fig. 2(b). The rotational quantum numbers of the absorption systems assigned are shown with field region of the system indicated. (b) A high field absorption system of NO_2 at $311 \mu\text{m}$. The observation of at least 26 triplets in the parallel spectrum indicates that one N value is at least 13. The observation of 58 triplets (some unresolved) in the perpendicular transition indicates the smaller N value is at least 14. No rotational assignment has been made of this system.

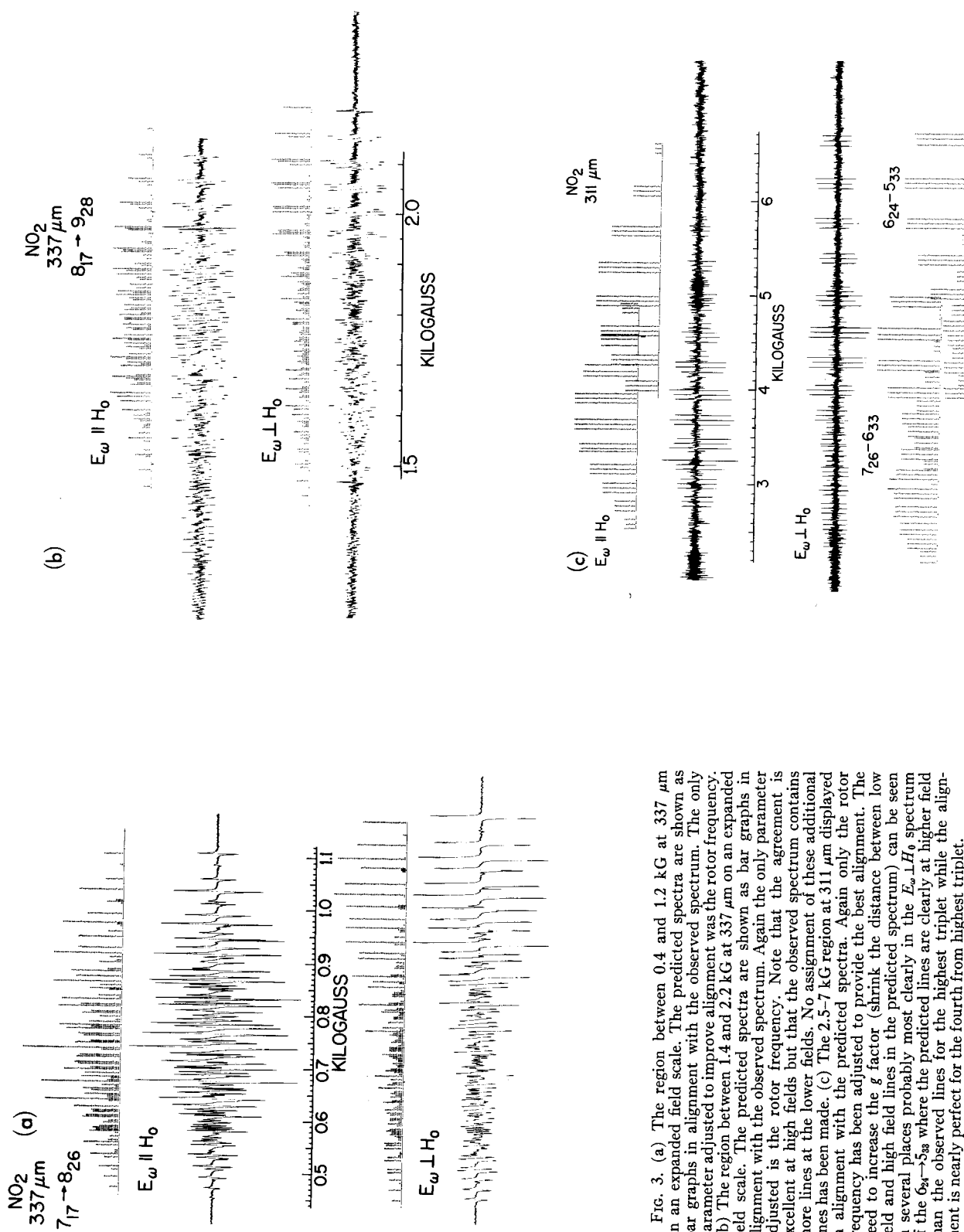


FIG. 3. (a) The region between 0.4 and 1.2 kG at $337 \mu\text{m}$ on an expanded field scale. The predicted spectra are shown as bar graphs in alignment with the observed spectrum. The only parameter adjusted to improve alignment was the rotor frequency. (b) The region between 1.4 and 2.2 kG at $337 \mu\text{m}$ on an expanded field scale. The predicted spectra are shown as bar graphs in alignment with the observed spectrum. Again the only parameter adjusted is the rotor frequency. Note that the agreement is excellent at high fields but that the observed spectrum contains more lines at the lower fields. No assignment of these additional lines has been made. (c) The 2.5-7 kG region at $311 \mu\text{m}$ displayed in alignment with the predicted spectra. Again only the rotor frequency has been adjusted to provide the best alignment. The need to increase the g factor (shrink the distance between low field and high field lines in the predicted spectrum) can be seen in several places probably most clearly in the $E_\omega \perp H_0$ spectrum of the $6_{21} \rightarrow 5_{20}$ where the predicted lines are clearly at higher field than the observed lines for the highest triplet while the alignment is nearly perfect for the fourth from highest triplet.

TABLE III. Predicted rotational transitions near the HCN laser lines (MHz).

	Transition	ν_0^a	$\Delta\nu_{cd}^b$
311 μm (964 313.4)	$6_{2,4} \rightarrow 5_{3,3}$	979 336.0	-4 836.7
	$7_{2,6} \rightarrow 6_{3,3}$	954 200.0	-4 802.6
	$9_{1,9} \rightarrow 10_{2,8}$	950 195.4	-954.3
	$10_{1,9} \rightarrow 11_{2,10}$	939 919.6	-933.2
	$12_{1,11} \rightarrow 13_{2,12}$	982 619.5	-865.9
	$24_{3,21} \rightarrow 23_{4,20}$	970 475.1	-10 753.8
	$25_{3,23} \rightarrow 24_{4,20}$	945 911.0	-10 514.8
	$34_{0,34} \rightarrow 35_{1,35}$	956 954.8	-228.8
	$36_{0,36} \rightarrow 37_{1,37}$	996 833.7	-355.2
	$39_{1,39} \rightarrow 39_{2,38}$	960 834.1	-698.9
337 μm (890 760.7)	$7_{1,7} \rightarrow 8_{2,6}$	893 154.3	-1 015.4
	$8_{1,7} \rightarrow 9_{2,8}$	895 856.4	-991.1

^a Using the centrifugal distortion constants of Ref. 5.

^b ν_0 including centrifugal distortion minus ν_0 from the rigid rotor.

calculate the Zeeman spectrum of NO_2 . The program was organized in the following way. The input data consisted of the rotational constants, hyperfine coupling constants, rotational quantum numbers, central magnetic field H_0 , a magnetic field interval ΔH , and the laser frequency¹⁸ ν_L . The first step was the calculation of the energy levels of both rotational levels involved in the transition at $H_0 - \Delta H$, H_0 , and $H_0 + \Delta H$.

In the calculation of the energy levels the problem was set up in the Wang basis (i.e., rotational wavefunctions of the correct symmetry for the asymmetric rotor, but appropriate to $\kappa = -1$). The coupling scheme used (which is irrelevant to the results) was $|N_{K-K+}, S, J, I, F, M_F\rangle$. The quantum numbers J and F are not even approximately good quantum numbers. The only matrix elements off-diagonal in N_{K-K+} included in a Van Vleck perturbation were

$$\langle N_{K-K+}, S, J = N + 1/2, I, F, M_F | H | (N + 1)_{K-K+}, S, J = N + 1/2, I, F, M_F \rangle,$$

and

$$\langle N_{K-K+}, S, J = N - 1/2, I, F, M_F | H | (N - 1)_{K-K+}, S, J = N - 1/2, I, F, M_F \rangle.$$

These same elements were considered in the original treatment of NO_2 .⁶

It was found that inclusion of all terms off-diagonal in N_{K-K+} in a Van Vleck perturbation (as was done in later work on NO_2)⁹ required an inordinate amount of computer time. Note that the second order effects of rotational asymmetry are not included.

In the energy calculation the fact that M_F is a good quantum number was used. Each Hamiltonian matrix for a given rotational level and M_F was set up and

diagonalized. The transformations that diagonalize the Hamiltonian matrices were saved.

Next the direction cosine matrices between the two rotational levels involved were computed. These were set up in the $|N_{K-K+}, S, J, I, F, M_F\rangle$ basis and transformed to the energy basis by the saved transformations.

The absorption intensity is proportional to the direction cosine matrix elements squared. Therefore the next step in the calculation was to search each direction cosine matrix at the central field H_0 ($\langle M_F | \lambda_z^b | M_F \rangle$ for parallel selection rules, $\langle M_F' | \lambda_x^b | M_F \rangle$ for perpendicular selection rules) for elements larger in magnitude than a certain critical value. When such elements were found the frequency of the corresponding transition was computed and compared to a frequency interval (previously decided upon) about the laser frequency. If the transition frequency is in the interval, the magnetic field H at which the transition frequency equals the laser frequency was computed by quadratic interpolation using the frequencies at the three fields $H_0 - \Delta H$, H_0 , and $H_0 + \Delta H$. The intensity at the resulting field was then computed by a similar quadratic interpolation.

ASSIGNMENT OF THE SPECTRA

The first step in the assignment of the spectra was the prediction of the rotational transitions of NO_2 in the neighborhood of each laser line. For this purpose the rigid rotor approximation was made. The next step was the computation of the frequencies of likely rotational transitions including the effects of centrifugal distortion. The results of these calculations are shown in Table III. As can be seen the centrifugal distortion correction can be quite large.

From the results shown in Table III it seemed likely that the low field transitions (500–1100 G) at 337 μm arose from the $7_{17} \rightarrow 8_{26}$ transition, while those around 1900 G could still be part of $7_{17} \rightarrow 8_{26}$ or could arise from $8_{17} \rightarrow 9_{28}$. The lines between 2500 and 6500 G at 311 μm could arise from either or both of the $7_{26} \rightarrow 6_{33}$ and $6_{24} \rightarrow 5_{33}$. These results were verified with further calculation using the spectrum computation program described above, and are shown summarized in Fig. 3. The spectrum prediction computations show that the absorptions between 2500 and 6500 G at 311 μm arise from both the $7_{26} \rightarrow 6_{33}$ and the $6_{24} \rightarrow 5_{33}$ with the lower field absorptions belonging to $7_{26} \rightarrow 6_{33}$ and the higher field belonging to $6_{24} \rightarrow 5_{33}$. The two systems overlap around 4000 G. The strong absorptions left unaccounted for by these four rotational assignments are a number of lines mixed in with the $8_{17} \rightarrow 9_{28}$ around 1400 G at 337 μm , the system between 4 and 6 kG at 337 μm , the system between 0.7 and 3.2 kG at 311 μm , and the beautiful system just above 10 kG at 311 μm . This latter system must have the larger $N \geq 13$ because there are at least 26 triplets in the $\Delta M = 0$ spectrum. No

TABLE IV. Expected values of parameters from previous work and results of least square fitting.

Parameter	Previous value	Uncertainty in previous value used in diagnostic least squares		Results of fitting		
		First least squares	Second least squares	First least squares	Second least squares	Second least squares uncertainty
Electron spin ^a						
(0) _g ^(S)	1.9997 ^d	0.0007	0.007	... ^f	2.013	0.002
(aa) _g ^(S)	-0.0087 ^d	0.0007	0.007	...	-0.010	0.003
(cc) _g ^(S)	0.0065 ^d	0.0007	0.007	...	0.0025	0.006
Rotational g-tensor ^b						
(0) _g ^(N)	0	1.4	1.4	-0.9 ^f	-0.0	1
(aa) _g ^(N)	0	1.4	1.4	+0.5 ^f	-0.2	0.8
(cc) _g ^(N)	0	1.4	1.4	-1.1 ^f	+0.3	0.7
Rotor frequencies ^c						
6 _{2,4} →5 _{3,3}	979 336.0 ^e	200	200	979 230.3	979 351.7	20
7 _{2,6} →6 _{3,3}	954 200.0 ^e	200	200	954 047.2	953 981.2	10
7 _{1,7} →8 _{2,6}	893 154.2 ^e	200	200	893 209.1	893 232.1	2.5
8 _{1,7} →9 _{2,8}	895 856.4 ^e	200	200	895 928.6	895 962.6	5
				First least squares	Second least squares	
$\Sigma(H_{\text{obs}} - H_{\text{calc}})^2$				146. ^g	3.1 ^g	

^a In units of the Bohr magneton.

^b In units of the nuclear magneton ($\mu_N \approx \mu_B/1836$).

^c In megahertz.

^d As quoted in Ref. 6.

^e Calculated from the rotational and centrifugal distortion constants of Ref. 6.

^f These parameters are not really determined in this fit.

^g (G)².

obvious candidate appears. Because the computational time required for high N transitions is very large, no Zeeman spectrum predictions were attempted to search for an assignment of this system or the other unassigned systems.

The comparisons of the predicted and observed spectra are shown in Fig. 3. In making a predicted rotational transition correspond to the above spectrum, the only parameter adjusted was the rotor frequency. These adjustments could be as great as 200 MHz indicating a considerable uncertainty in the centrifugal distortion shifts. From Fig. 3 it is clear that there can be little doubt about the assignments.

SELECTION RULES FOR THE TRANSITIONS

It may be surprising that these transitions have been identified as electric dipole transitions. It is well known that decoupling of the angular momentum occurs in strong magnetic fields and that the appropriate basis set is $|N_{K-K_+} M_N S M_S I M_I\rangle$. The Zeeman term then becomes

$$E_Z = 2\mu_B M_S H. \quad (10)$$

The electric dipole selection rules become $\Delta M_S = 0$ and the electric dipole allowed transition frequencies do not vary with the field so that no laser magnetic resonance spectrum is observable.

Before concluding from the above argument that the electric dipole transitions can not be observed and the assignments arrived at must be nonsense, it is prudent to examine the selection rules for magnetic dipole transitions. The intensity of magnetic dipole transitions between two levels is proportional to the square of the magnetic dipole moment matrix element between the two levels. From Eq. (2) the magnetic dipole moment operator can be seen to be the sum of three terms corresponding to \hat{H}_S , \hat{H}_N , and \hat{H}_I . However, \hat{H}_S is about 2000 times larger than \hat{H}_N or \hat{H}_I and it seems unlikely that transitions which are allowed by matrix elements of \hat{H}_N (or \hat{H}_I) will be strong enough to be observed. The selection rules for \hat{H}_S in the completely uncoupled scheme are $\Delta N = 0$, $\Delta K_- = 0$, $\Delta K_+ = 0$, $\Delta M_N = 0$, $\Delta M_S = \pm 1$. Thus only transitions between the Zeeman components of a single rotational level are allowed and such transitions could not be found at frequencies as high as 800 GHz.

We are convinced that the transitions observed here are electric dipole allowed and have $\Delta M_S = \pm 1$. This is possible because decoupling is not complete due to the large value of the spin rotation interaction ($A_s = 5.46$ GHz). The transition frequency, therefore, will depend on magnetic field and laser magnetic resonance with electric dipole selection rules is possible.

FITTING THE SPECTRUM

As was mentioned previously, the magnetic field was measured accurately for several of the Zeeman components. These measurements along with the assignments are listed in Table I.

It is of interest to see if the spectrum can be fitted with the Zeeman Hamiltonian Eq. (2), and to determine as many of the constants in the Hamiltonian as possible. From Table II it is clear that at most only H_S and H_N should be needed to fit the spectrum. This means that there is some hope of determining the first six parameters listed in Table II. Since the rotor frequency of each rotational transition is to be adjusted and there are four rotational transitions, the spectrum is to be fitted with ten parameters. With so few observations to be fitted by so many parameters, it appears dubious that the parameters will be well determined.

In order to study the behavior of the least squares process, a method called diagnostic least squares was employed.¹⁹ In this procedure, before the fitting is attempted each parameter is assigned a guessed value and an uncertainty based on physical intuition. In a very crude sense what takes place is that no change is made in a parameter in the fitting process unless the parameter is better determined by the data being fitted than by the original guess. If the parameter is changed its new value is completely determined by the data. The actual meaning of the fitting process has been discussed elsewhere.¹⁹ In Table IV the guessed values of the ten parameters and their uncertainties are listed. The relatively large uncertainties of 200 MHz in the rotor frequencies were chosen because the low J line $2_{02} \rightarrow 1_{11}$ was off 31 MHz from the centrifugal distortion prediction.⁹ For the components of the $g^{(S)}$ tensor the uncertainty should be fairly small (~ 0.0007) because the electron spin resonance of NO_2 has been observed in radiation damaged NaNO_2 ²⁰ and is in good agreement with theory.^{6,17}

In the least squares the field H , at which a particular transition is observed, is considered to be a function of $(0)_g^{(S)}$, $(aa)_g^{(S)}$, $(cc)_g^{(S)}$, $(0)_g^{(N)}$, $(aa)_g^{(N)}$, $(cc)_g^{(N)}$, and ν_0 (the frequency of the particular rotational transition). The nonlinearity of the dependence of H on these parameters is removed by the usual technique of Taylor series expansion so that what is required as input to the least squares procedure is a matrix of derivatives of the various magnetic field values with

respect to the various Zeeman Hamiltonian parameters and a vector of $H_{\text{obs}} - H_{\text{calc}}$ where H_{calc} is calculated from a set of initial values of the parameters. The derivatives of H with respect to the parameters were obtained by calculating the transition frequency and its derivatives at the observed value of H using the same approach as in the spectrum prediction calculations. The implicit function theorem was then used to evaluate derivatives of H

$$\left(\frac{\partial H}{\partial (0)_g} \right)_\nu = - \left(\frac{\partial \nu}{\partial (0)_g} \right)_H / \left(\frac{\partial \nu}{\partial H} \right)_{(0)_g} \quad (11)$$

The fact that the Zeeman Hamiltonian is homogeneous of order 1 in H , allowed the calculation of the derivative of the frequency with respect to H from

$$\frac{\partial \nu}{\partial H} = \left[(0)_g \frac{\partial \nu}{\partial (0)_g} + (aa)_g \frac{\partial \nu}{\partial (aa)_g} + \dots \right] / H. \quad (12)$$

The quantities $H_{\text{obs}} - H_{\text{calc}}$ were obtained from

$$H_{\text{obs}} - H_{\text{calc}} = -(\nu_L - \nu_{\text{calc}}) (\partial \nu / \partial H)^{-1}. \quad (13)$$

When the guesses of Table IV are used in diagnostic least squares fit of the data of Table I, it is found that six of the ten parameters should be better determined by the data than by the guesses. These parameters are the four rotor frequencies and two of three possible linear combinations of the rotational g tensor components. However, the fit is very poor,

$$\sum (H_{\text{obs}} - H_{\text{calc}})^2 = 146(\text{G})^2.$$

In other words the guesses of Table IV are incompatible with the observed spectrum, unless there are errors of several gauss in the field measurements.

A second least squares was carried out increasing the uncertainty in the electron spin g tensor by a factor of 10. The diagnostic least squares results indicate that eight of the ten parameters are now better determined by the data than by the guesses. The two undetermined linear combinations of parameters are primarily $(cc)_g^{(S)}$ and $(0)_g^{(N)}$ although $(aa)_g^{(N)}$ and $(cc)_g^{(N)}$ are poorly determined. The fit is much better, $\sum (H_{\text{obs}} - H_{\text{calc}})^2 = 3.1(\text{G})^2$. The parameters resulting from the fitting are given in Table IV.

The principal change in going from the first fit to the second is that $(0)_g^{(S)}$ increases by 0.015. The $H_{\text{obs}} - H_{\text{calc}}$ for both fits are reported in Table I. Looking at these numbers it is clear that there appears to be something wrong with the field scale in the first least squares or alternatively $(0)_g^{(S)}$. Experimental checks of the field measurement have been made and no source of systematic error in the field scale can be found.

On the other hand no reason for a large change in the isotropic part of the g tensor on going from the solid phase to the gas phase has been found. Possibly a

dependence of A_s on K could result in an apparent increase in $(0)_g^{(S)}$.

The anisotropic component $(aa)_g^{(S)}$, as determined by the second fit, has essentially the same value as in the solid phase.

CENTRIFUGAL DISTORTION

The previous work on NO₂^{6,9} resulted in the determination of seven rotor frequencies for ¹⁴N¹⁶O₂. The four rotor frequencies determined here give a total of 11 rotor frequencies which can be fitted with rotational and centrifugal distortion constants. There are three rotational constants, five fourth order centrifugal distortion constants, and seven sixth order centrifugal distortion constants, a total of fifteen parameters, to be determined. Further it is possible that one or more eighth order centrifugal distortion constants are important. There seems little hope of significantly improving the centrifugal distortion treatment by including the additional four rotor frequencies.

SUMMARY

Laser magnetic resonance spectra of NO₂ have been observed using the 311 and 337 μm HCN laser lines as the source. Hyperfine components of four rotational transitions have been assigned. Although the qualitative agreement between the observed and predicted spectra is excellent, the value of the isotropic electron spin g factor required to fit the data quantitatively is significantly larger than that found in the solid state. The anisotropic electron spin g factor which is determined agrees well with that found in the solid state. The four additional rotor frequencies obtained increase

the number of accurately known rotor frequencies for ¹⁴N¹⁶O₂ to 11. This is still an insufficient number to determine the centrifugal distortion constants.

* This work supported by Grant C-071 of the Robert A. Welch Foundation and National Science Foundation Grant GP6305X.

¹ K. M. Evenson, H. P. Broida, J. S. Wells, R. J. Mahler, and M. Mizushima, *Phys. Rev. Letters* **21**, 1038 (1968).

² K. M. Evenson, J. S. Wells, and H. E. Radford, *Phys. Rev. Letters* **25**, 199 (1970).

³ K. M. Evenson, H. E. Radford, and M. Moran, *Appl. Phys. Letters* **18**, 426 (1971).

⁴ M. Mizushima, K. M. Evenson and J. S. Wells, *Phys. Rev. A* **5**, 2276.

⁵ G. R. Bird, *J. Chem. Phys.* **25**, 1040 (1956).

⁶ G. R. Bird, J. C. Baird, A. W. Jache, J. A. Hodgeson, R. F. Curl, A. C. Kunkle, J. W. Bransford, J. Rastrup-Andersen, and J. Rosenthal, *J. Chem. Phys.* **40**, 3378 (1964).

⁷ J. A. Hodgeson, E. E. Sibert, and R. F. Curl, *J. Phys. Chem.* **67**, 2833 (1963).

⁸ L. Esterowitz and J. Rosenthal, *J. Chem. Phys.* **40**, 1986 (1964).

⁹ R. M. Lees, R. F. Curl, and J. G. Baker, *J. Chem. Phys.* **45**, 2037 (1966).

¹⁰ P. D. Foster, J. A. Hodgeson, and R. F. Curl, *J. Chem. Phys.* **45**, 3760 (1966).

¹¹ G. R. Bird, G. R. Hunt, H. A. Gebbie, and N. W. Stone, *J. Mol. Spectry.* **33**, 244 (1970).

¹² L. O. Hocker and A. Javan, *Phys. Letters* **25A**, 489 (1967).

¹³ C. C. Lin, *Phys. Rev.* **116**, 903 (1959).

¹⁴ R. F. Curl and J. L. Kinsey, *J. Chem. Phys.* **35**, 1758 (1961).

¹⁵ W. M. Tolles, J. L. Kinsey, R. F. Curl, and R. F. Heidelberg, *J. Chem. Phys.* **37**, 927 (1962).

¹⁶ W. Hüttner, M. Lo, and W. H. Flygare, *J. Chem. Phys.* **48**, 1206 (1968).

¹⁷ R. F. Curl, *Mol. Phys.* **9**, 585 (1965).

¹⁸ It will become apparent from the following discussion that this program does not include centrifugal distortion shifts of the rotational frequency or even second order effects of asymmetry. These effects were computed elsewhere and introduced by correcting the laser frequency ν_L by subtracting these effects.

¹⁹ R. F. Curl, *J. Comput. Phys.* **6**, 367 (1970).

²⁰ H. Zeldes and R. Livingston, *J. Chem. Phys.* **35**, 563 (1961).